SZENT ISTVÁN UNIVERSITY

Building integrated shell-structured solar collectors

Thesis of PhD Dissertation

by

István Fekete

Gödöllő, Hungary
2015

Doctoral school denomination: Mechanical Engineering PhD School

Science: Energetics of Agricultural and Environmental Engineering

Leader: Prof. Dr. István Farkas
Dr. of Technical Sciences
Faculty of Mechanical Engineering
Szent István University, Gödöllő, Hungary

Supervisor: Prof. Dr. István Farkas
Dr. of Technical Sciences
Institute for Environmental Engineering Systems
Faculty of Mechanical Engineering
Szent István University, Gödöllő, Hungary

…… ……

Affirmation of the Doctoral School Leader Affirmation of supervisor

CONTENTS

1. INTRODUCTION AND OBJECTIVES

The solar panels and installation of choosing, aesthetics significant factor. The placement, mostly houses and buildings roof. Thus, a design plan on which the look of the buildings do not convert, but it is possible the active utilization of solar energy.

To access the building's structural elements integrated collectors are required to carry out the following tasks.

1. To examine the development of mathematical models, solar radiation energy attenuation from the surface of the material and in the deeper layers of thermal conductivity process of conducting a theoretical simulation of processes, more accurate data needed to advance the development of the actual experimental elements.
2. Test pieces of different design and surface coating layer structures. With their help, I will examine the elements in the real environment of solar radiation attenuation, reflectance, thermal equilibrium processes.
3. Solar system bodies develop, theoretical calculations, the simulation results and the measurements carried out on the basis of specimens, which also function as structural elements as well.
4. Create a testing device which is suitable for the changes in the factors affecting the absorption of solar radiation followed. Suitable for a collector to be measured in different orientations and angles of incidence, thermal and comparative measurements of the set to perform.
5. Development of the method for calculating the efficiency of solar collectors operating conditions. The design of accurate measurements, using appropriate mathematical methods to study the replacement of standard laboratory assessments.
6. I study the effect of temperature measuring instruments to determine the accuracy of the collector efficiency curve. In order to eliminate the disproportionately costly certification procedures.
7. An economic evaluation analysis calculations. Expansion of economic processes payback technical characteristics, the economic applicability of solar hot water and central heating backup in the area.

2. MATERIAL AND METHODS

In this section, I present the material and methods that you can use the new type of structural element can be utilized, shell construction, solar collector construction, development and testing took place.

2.1. Modelling, simulation methods

Solar collectors for thermal conditions, structural elements, the heat transfer processes modelling and simulation to analyse. The task of the collector without covering thermal modelling. The mathematical model is necessary to examine the conditions of application of the model equations for thermal collectors and bodies will choose the other calculations on the basis of compliance.

2.1.1. The equations of heat radiation

The *thermal radiation (radiation)* is an energy transmission mode, when one of the body of the energy will be transferred to another form of electromagnetic waves (EMW s). Planck justified assumption that the particles are vibrating movement during the energy nanophysics valid, ie the particles are formed, each of oscillators oscillating at different frequencies corresponding to the characteristic of them only frequency:

$$E = h\,\nu\ , [J], \tag{2.1}$$

energy can pick up units and may return to power. In equation (2.1) h is Planck's constant (h = 6,63·10-34 J·s), ν individual oscillators oscillation frequency [1/s]. Based on this, statistically, the Boltzmann distribution using the Planck's radiation law:

$$E(\nu) = \frac{8\pi h \nu^3}{c^3} \frac{d\nu}{e^{\frac{h\nu}{kT}} - 1}, \quad [J] \tag{2.2}$$

where, k is the Boltzmann constant (k = 1,38·10^{-23} J/K), c speed of light [m/s].

Because of the surroundings along the thermal radiation of bodies (they are not absolute 0 degrees), each body is constantly EMN s reach. Part of the reason for coming to customize EMN surface is reflected (reflection), other portion is absorbed in the body (absorption) and passes through the body (transmission). Thus, the electromagnetic radiation from the entire customized E the following balance equation:

$$E = E^r + E^a + E^t\ , \tag{2.3}$$

wherein, E^r is the relected (reflected), E^a is absorbed (adsorbed) and E^t is transmitted (transmission) of electromagnetic radiation.

In summary, the bodies of two properties affect radiative heat flow:

- *the temperature* at which, due to the fourth power of the temperature increase, a greater extent increasing the transmitting power, and
- *the surface finish,* which displays the specific emission coefficient (ε).

2.1.2. The equations of heat conduction

The *thermal conductivity (or conduction)* the form of energy exchange, when a result of the temperature difference energy reaches warmer (higher temperature) from parts of the material in the cooler (lower temperature) parts without the material particles is occupied relative to one another about their altered.

Non-steady-state heat conduction in solids

The non-stationary (unsteady) processes in the body cools or warms relate. This phenomenon may be caused by the fact that the body is different from the temperature of its environment with a temperature or heat source/sinks have. The non-steady (transient) for the temperature distribution in the body is changing in time, ie

$$\frac{\partial T}{\partial \tau} \neq 0. \tag{2.4}$$

A reconciliation of the ignored solutions can be said that the body temperature of each case varies exponentially decreases exponentially case of cooling, warming the event is growing exponentially.

2.1.3. The equations of heat transfer

Heat transfer (convection) in the case where the surface and between contiguous fluid (gas or liquid) of the solid material, as a result the temperature difference energy exchange takes place. Heat flux between the fluid and the surface of the solid can be expressed in Newton's heat transfer equation:

$$\dot{Q}_{á} = \alpha A (T_w - T_f), \tag{2.5}$$

$$\underline{\dot{q}}_{á} = \alpha \, (T_w - T_f), \tag{2.6}$$

where, $\dot{Q}_{á}$ the handover heat flux [W], $\underline{\dot{q}}_{á}$ the transfer heat flux density [W/m^2], α heat transfer coefficient [W/(m^{2}K)], A the heat transfer surface [m^2], T_w the solid surface temperature [K], T_f a the ambient fluid temperature [K].

2.2. Mathematical modelling of building integrated solar collector

In my dissertation I use to perform the calculations in MATLAB special program system, developed to perform numeric calculations and is also a programming language. The building integrated solar collectors thermal behaviour of elements was analysed using simulation method. The thermal conductivity of differential equations based, one component of the energy transfer to the next one, the space part of the energy balance of in- and outgoing heat transfer material is formed depending on the volume of flow.

To perform the mathematical simulation (Matlab) in the following equations prescribing necessary: the tile element surface to the environment, the tile element volume, mass, the tile element reaching "useful" solar radiation intensity, heat balance between the water and the collector element, the collector element and the environment heat balance between the working fluid on the collector element (water) the temporal change amount of heat, and the collector element summing equations temperature and the working fluid temperature.

2.3. Specimen testing method

In my dissertation it was necessary to examine the structural materials of solar radiation absorption and the surface temperatures developments, their dynamics over time.

The measurements were carried out in different shaped surfaces to determine the actual absorption of solar radiation energy. For the preparation of specimens for measurement are shown in Figure 2.1.

Fig. 2.1. Surface temperature measurement layout

The experiments measuring instruments

To measure the surface temperature of the infrared thermometer was used. The infrared temperature measurement principle because of the temperature of objects can be checked. Temperature measurement range -30, +260 °C, temperature resolution of 0.1 °C and accuracy of ± 2% ± 2 °C. Temperatures were measured during the surface, 10 mm depth, determining capillary tube thermometer clocks applied, have a resolution of 1 degree Celsius, so that the reading accuracy of ± 0.5 °C.

2.4. The development of measuring system

The necessary investigations were carried out theoretical calculations to demonstrate the self-designed and manufactured test equipment. Two circular (solar and hot water) installation ensures proper separation and improved control. The connection between the two circuit provides an external heat exchanger. The three-speed circulation pumps using. The connections implemented using copper pipes.

2.5. Determination method of solar collector efficiency

Necessary to measure the fluid warming in the collector. The measurement of the intensity of solar radiation and in the collector current of the flowing liquid volume as a function of. After that context we are looking for and the size of the solar collector thermal efficiency of the surface of the solar radiation falling between global.

The test parameters describing the phenomenon efficiency (η), which describes the differences in thermal efficiency of the collector. The test parameters can be factors: solar radiation intensity (I_g), the air around the collector temperature (T_a), the collector flowing heat extraction fluid medium temperature (T_m), the inlet collector fluid temperature (T_{in}), the collector outlet fluid temperature (T_{out}) , the collector medium and the temperature difference between the ambient temperature (T_m-T_a).

The amount of fluid flowing through the collector hot water meter is determined using. The measuring accuracy of ± 0.1 liters.

The measured data to evaluate the factorial experimental approach is available. This method is commonly used in the research literature, however, to determine the solar efficiency function has not been used before.

The application of the following objectives:

- the effect of the factors listed above the solar collector efficiency on the change, leaving negligible factors,

- establish a decisive factor values (η) than the phenomenon extreme value,

- interpretation of the given range, and determining a change in the analysed factors (G, ΔT) function relationship of efficiency.

2.6. Data processing system and method

Measurement is to be achieved during processing large amounts of data capture, evaluation of computer-assisted methods, that will be suitable for the preparation of subsequent analyses. We have prepared a data acquisition and analysis software that helps carry out further work.

Temperature distribution measurement and evaluation

The collector surface temperature distribution is difficult to measure using conventional temperature measuring devices. Therefore, the temperatures detect and verify the modelled values calculated infrared camera recordings were used. Infrared images of the software accuracy ± 0.1 °C and Figure 2.2. shows the recording features.

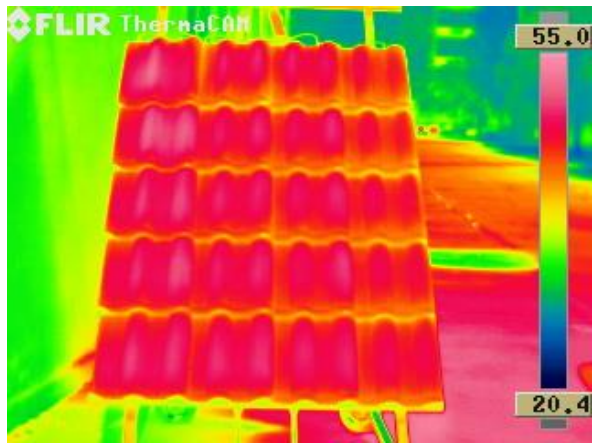

Fig. 2.2. Measured surface temperature distribution of elements

During the evaluation of thermal images temperatures not identified, but radiation intensity levels. The modern infrared cameras setting can be chosen freely, but are recommended for detection usual settings (colour scale) also examples of colour classification right side of Fig. 2.2.

3. RESULTS

In this chapter, I introduce them to new scientific achievements, methods, procedures and limits of the applicability of these findings shall communicate that lead to the development of a new type of solar collectors is done.

3.1. Modelling of building integrated solar collector

The literature review confirms that people with solar collectors appreciated not only by their usefulness, but also according to aesthetic considerations. In my research this principle, been built. In addition to traditional solar collectors to examine this area, how is a viable solution when the building's structural elements can also be used to capture solar energy (Fig. 3.1).

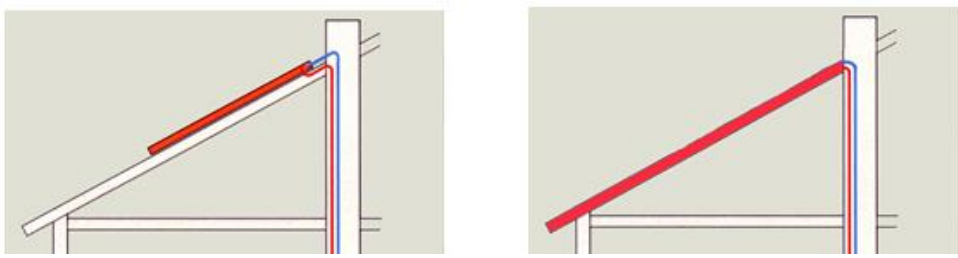

Fig. 3.1. The traditional and advanced structure design of solar collector

The mathematical model and simulation of solar radiation energy absorption and thermal conductivity processes

The thermal conductivity of differential equations based, one component of the energy transfer to the next one, the space part of the energy balance of inputs and outputs depending on the heat transfer material is formed of flow (Fig 3.2).

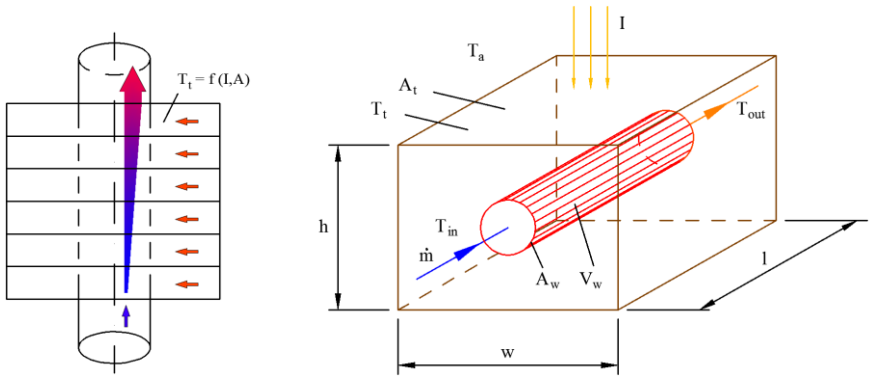

Fig. 3.2. Structure and heat balance scheme of tile element

The building integrated solar collector model of the solar thermal technology development, environmental variables must be entered in addition to the geometry data of the physical characteristics of the materials used.

The next mathematical equations necessary for the simulation:

$$\dot{T}_t = \frac{I A_t + k_{ta} A_{ta} (T_a - T_t) - k_{wt} A_w (T_t - T_{out})}{c_t m_t}, \tag{3.1}$$

$$\dot{T}_{out} = \frac{k_{wt} A_w (T_t - T_{out}) - \dot{m}_w c_w (T_{out} - T_{in})}{c_w \rho_w V_w}. \tag{3.2}$$

Establishment of solar collectors outlet temperature of the working fluid by summarizing sequential thermal equilibrium state of the elementary particles can be observed. Based on equations (3.1 - 3.2) derived from mathematical simulation process is shown in Fig. 3.3, including the following notations:

$$U[1] = \dot{T}_t \; ; \; U[2] = \dot{T}_{out} \; ; \; U[3] = T_{in} . \tag{3.3}$$

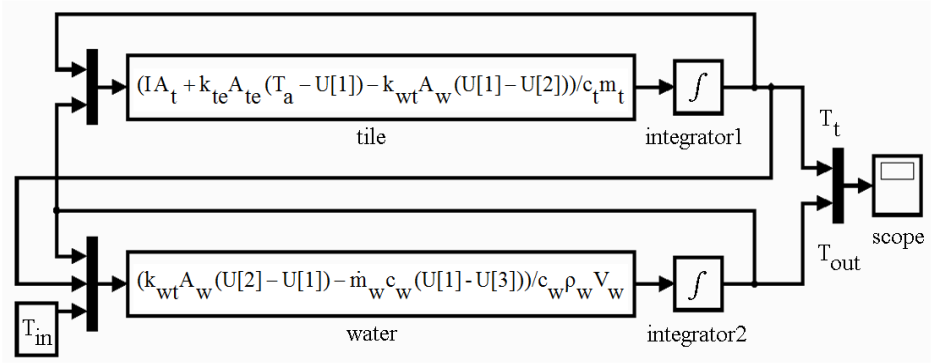

Fig. 3.3. Matlab realization of the tile collector model

The table 3.1 shows the parameter values used in the experiment and in the course of Matlab simulation.

Table 3.1. Parameters values used for simulation

Parameters	Values	Parameters	Values	Parameters	Values
l	2.5 m	c_t	900 J/kgK	$\dot{m}$	0.01 kg/s
d_w	0.005 m	c_w	4196 J/kgK	ρ_w	1000 kg/m^3
ρ_t	2000	w	0.02 m	T_a	20 °C
h	0.015 m	I	600 W/m^2	T_{in}	18 °C
k_{te}	20 W/m^{2}K	k_{wt}	150		

The temperature distributions in the shell-structured tiles calculated by simulations were first analysed. Fig. 3.4 shows the warming process until steady state is reached. Based on the afore-mentioned parameters, the maximum available tile surface temperature difference (ΔT_t) is about 27 °C, the outlet fluid difference temperature (ΔT_{out}) is about 25 °C over, and the inlet temperature (T_{in}) is 18 °C.

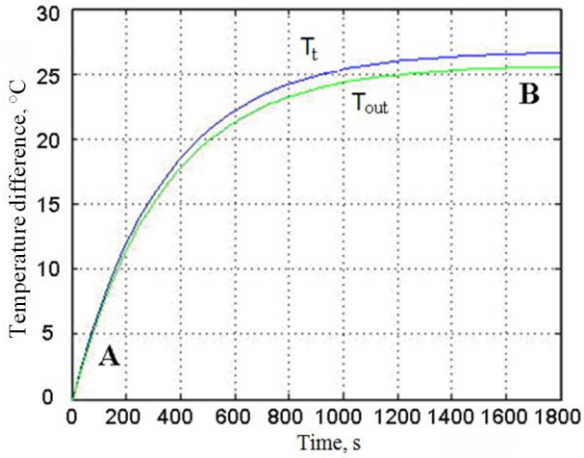

Fig. 3.4. Calculated temperature differences of tile and outlet working fluid

Parameter sensitivity study

The simulation results can be used to determine the parameters with the most influence and operational variables of the solar tile system, which can be used in the development of a new collector structure. In Table 3.2, the parameters with the most influence are shaded along with some practical notes.

Table 3.2. The list of the influencing parameters (most influence are shaded)

Parameters	Notes
length of tube (l):	can be used for optimization of heat transfer, number of serial elements
diameter of tube (d_w):	can be used for optimization of flow resistance, $d_w < h$; $d_w < w$; d_w max. is about h/2 and w/2
mass flow rate of water ($\dot{m}$):	can be used for pump optimization
volume of tube (V_w):	can be used for optimization of heat transfer
surface of tube (A_w):	can be used for optimization of heat transfer
specific heat of working fluid (c_w):	can be considered as other than water
density of working fluid (ρ_w):	can be considered as other than water

3.2. Construction of shell-structured collector system

Use of different test materials

Measurements were carried out at different surfaces in order to compare the actual capture of solar radiation (Fig. 3.5). Constant temperature of the absorber surface (T_t) can be reached when the heat formed part of the incoming global radiation which is equal to the loss and the conveyed of heat energy.

$$I_g\,\alpha = E_{l1} + E_{l2} \cong f\,(T_t - T_a), \tag{3.4}$$

There is a proportionality factor (f), which depends not only on the heat transfer factors, but also on the absorbing surface material, its design and quality, furthermore it is influenced by temperature and distance from surrounding objects and wind speed. For example, the expected temperature of the rough, grey concrete surface with the following parameters: I_g = 600 W/m^2 incoming radiation, T_a = 20 °C ambient temperature, v = 1 m/s wind speed, k = 20 W/m^{2}K heat transfer coefficient (estimated value), α_{co} = 0,60 was as follows:

$$T_t = \frac{I_g\ \alpha_{co}}{k} + T_a = \frac{600\ 0{,}6}{20} + 20 \cong 38\,°C\,.$$

a) Black painted conc.

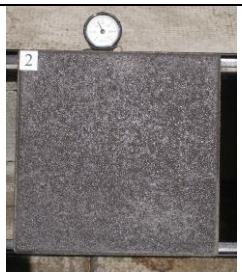

b) Lacquered concrete

c) Natural concrete

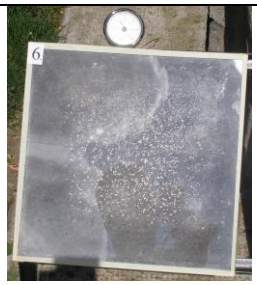

d) Plexigl.surf. (1 mm)

e) Thin plastic film surf.

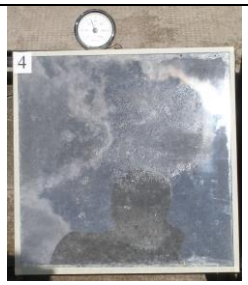

f) Glass surf. (2 mm)

Fig. 3.5. Different test examples

If the absorbing surface is covered with a transparent layer, the heat loss is reduced and the body temperature is increased under the same (I_g) incoming radiation. The surface temperature of the absorbing concrete, if there is a layer behind the glass, and it is insulated from its surroundings ideally with the parameters, incoming radiation I_g = 600 W/m^2, ambient temperature T_a = 20 °C, α_{conc} = 0.6, β = 5 W/m^{2}K, a_{gl} = 0.8:

$$T_t = \frac{I_g \; a_{gl} \; \alpha_{conc}}{\beta} + T_a = \frac{600 \; 0.8 \; 0.6}{5} + 20 \cong 77.6 °C$$

For example, if the conveyed specific performance E_c = 200 W/m^2. The surface temperature of the absorbing layer behind a glass was:

$$T_t = \frac{I_g \; a_{gl} \; \alpha_{co} - E_c}{\beta} + T_a = \frac{600 \; 0.8 \; 0.6 - 200}{5} + 20 \cong 37.6 °C$$

The resulting energy can be conveyed by liquid or air according to the type of collector working medium. Based on the above examples it can be stated that the uncovered surfaces behave more dynamically, while the covered surfaces showed a slower warming or cooling.

3.3. Thermal test of the solar tile collector

Positioning the solar collectors are usually done roof surface and because my main goal, replacing them with aesthetic reasons, so I used the concrete tile form. The concrete tile shape, size constraints were part of the heat exchanger construction, the positioning. The optimal distance pipe had to come back because the formal characteristics of the original concrete tiles. Manufacture of the heat exchanger of the first part, due to the better heat transfer processes is close to the planned absorber layer. However, this design has not been adequate for strength reasons (Fig. 3.6).

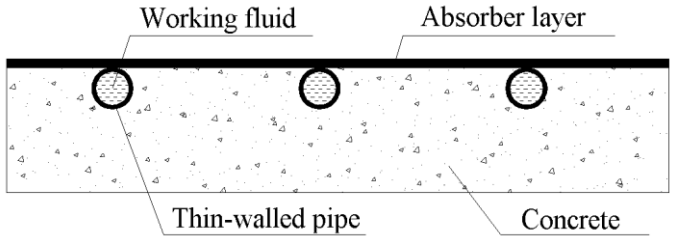

Fig. 3.6. The design of the concrete tile element layer

The converted corresponding load elements are made of a painted surface. Layer-planning design as shown in the Fig. 3.7.

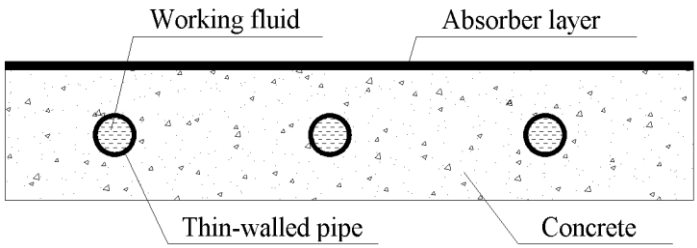

Fig. 3.7. The design of the concrete tile element layer

The actually produced tile shows the Fig. 3.8. Illustratively, the internal heat exchanger is placed in the interface. In the figure 3.9 shows the entire surface design.

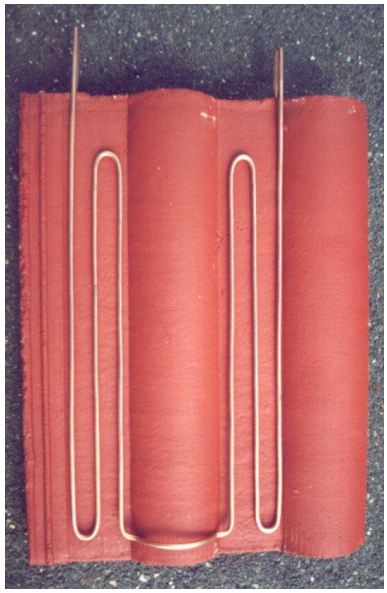

Fig. 3.8. The tile element design

Fig. 3.9. Surface of the collector (~2m^2)

Layout of the solar tile collector

Based on the modelling and simulation results a pilot system was designed and built. The system can serve to perform comparative measurements as expected in the simulation process. The tilt angle of the equipment varies between 30°- 45° and the azimuth angle is adjustable in the range of 0°-360°. In the figure 3.10a to create a complete pipe joint shown, and the closer fitting designs are shown in the figure 3.10b.

a) b)

Fig. 3.10. Rear surface of the tile collector.

Recording and storing of measurement data

The measurements are generated in large amounts of data capture, evaluation of computer-aided methods were performed, so the data will be used to create subsequent analyses.

Conformance the measured and calculated values

A representative image is shown in Fig. 3.11. The fluid enters at point A, and leaves the tile at point B. Point C shows the tile surface maximum temperature value, which is about 45 °C in the experiment. In this area, there is no heat extraction. The intensity of scale shows the approximate temperature values. The thermal image software accuracy was ± 0.1 °C.

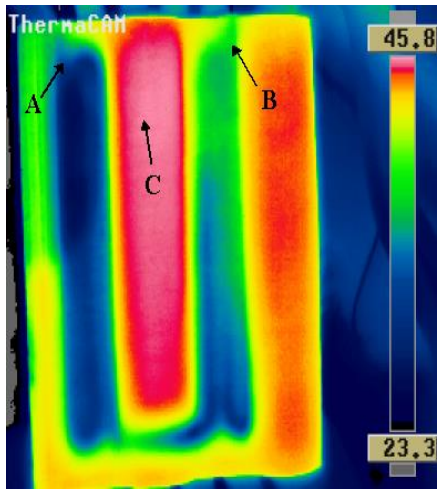

Fig. 3.11. Temperature distribution of a tile element

3.4. Method for determination of collector efficiency curve

Correlation has been found between changes in global solar radiation reaching the surface and the thermal efficiency of the collector. The test parameters describing the phenomenon efficiency (η), which describes the differences in thermal efficiency of the collector. The test parameters can be factors: solar radiation intensity (I_g), the air temperature around the collector (T_a), the collector flowing heat extraction fluid medium temperature (T_m), the inlet collector fluid temperature (T_{in}), the collector outlet fluid temperature (T_{out}) and the collector medium temperature difference between the ambient temperature (T_m-T_a). This pilot plan in connection with, among test parameters listed above, the radiation and the effect of temperature change experiment determined the efficiency. For the calculation of the radiation generalization of "G" were marked, the temperature difference is marked with "ΔT":

$$\eta = f(G, \Delta T). \tag{3.5}$$

The measured data to evaluate the factorial experiment was used.

Factor space analysis

The factors (G and ΔT) within the range of interpretation I took a test range ($\Delta T_{imin} - \Delta T_{imax}$), ($G_{imin} - G_{imax}$). This is necessary because the test results are valid within this range. The limiting factor space marked off sections of the experimental settings. As in my case is a two-factor experiment, so the vertices of the rectangle. Symbols used in the figure are in the literature (Fig. 3.12).

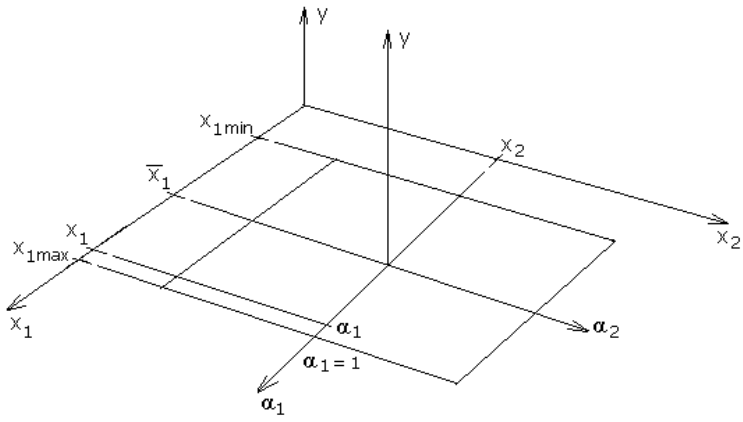

Fig. 3.12. Coordinate system placed in the centre of the factor space

The design of the evaluation of experimental results

In order to simplify the subsequent tests, the coordinate space factor for the transformation were carried out both factors. What began with a basic level needed to determine the factors:

$$\overline{G} = \frac{G_{\min} + G_{\max}}{2} \quad ; \quad \overline{\Delta T} = \frac{\Delta T_{\min} + \Delta T_{\max}}{2}. \tag{3.6}$$

Transformed factor name α_i, the test range was between -1 and 1. The factors G, ΔT and α_i (transformed factor) relationship as shown:

$$\frac{G - \overline{G}}{G_{\max} - \overline{G}} = \alpha_1 \quad ; \quad \frac{\Delta T - \overline{\Delta T}}{\Delta T_{\max} - \overline{\Delta T}} = \alpha_2 . \tag{3.7}$$

Completed the transformation of both factors, the test parameter η developed as follows:

$$\eta = f(\alpha_1, \alpha_2). \tag{3.8}$$

Thus, the transformed factors varied between -1 and 1, brought in experimental settings in these places (-), (+).

Examination of the model accuracy

Also, I did a series of measurements of the factor space centre. The results were as follows:

n	1	2	3	4	5
η_{0n}					

I received:

$\overline{\eta_0}$ s_0^2 values.

The approximate mathematical model to set up:

$$= \eta_0 - k\ a\ b_1k + b_2N + b_{12}kN.$$

On the results of the measurements I fitted function, based on the principle Legendre. The phenomenon of factors in linear model was approached:

$$\eta = b_0 + b_1G + b_2\Delta T + b_{12}G\ \Delta T. \tag{3.9}$$

The approximate margin of error functions:

I defined the variance in each experimental setting:

$$s_j^2 = \frac{1}{n-1}\sum_{i=1}^{n}(\eta_{ji} - \bar{\eta}_j)^2, \tag{3.10}$$

where, n the number of repetitions of the measurement (n = 5).

The variance of the approximate function:

$$s_\varepsilon^2 = \frac{\sum_{j=1}^{N} s_j^2}{N}. \tag{3.11}$$

Using the Student's test for the magnitude of error, at 5% significance level and 95% probability:

$$\Delta\varepsilon = t \cdot s_\varepsilon, \tag{3.12}$$

where, t = 2,015, according to Table F_1 (f = 5 belonging to the degree of freedom).

Examination of the variances identity

According to the Fisher test, variances in different experimental settings belong to the same theoretical variance if:

$$F_{kis} = \frac{s_{\max}^2}{s_{\min}^2} \le F_{tábl}, \tag{3.13}$$

where, $F_{tábl}$ value is 5,1.

If the value F_{kis} is less than the value in the table, according to the Fisher test, variances in different experimental settings belong to the same theoretical variance. If there is no matching, according to Fisher's test, Bartlett test will be applied.

$$\eta = \left[\bar{a}_0 + \bar{a}_1 \alpha_1 + \bar{a}_2 \alpha_2\right], \tag{3.14}$$

If this is met then the formula Δε margin of error, and 95% probability, describing the phenomenon. This is true in the assay range, and a function of the transformed factors.

Model accuracy test

As a first step we had to check that the simplified approach can also function describes the phenomenon within in margin of error. In a second step it is verified that the approximate function must consider the quadratic members.

$$\eta_{f0} = (\overline{\Delta T}_0, \overline{G}_0). \tag{3.15}$$

If there is in margin of error (Δε) within the η_{f0} the average value measured in this setting, then:

$$\eta_{f0} \pm \Delta\varepsilon, \tag{3.16}$$

in this case, the presence of the members assume in quadratic function approximation is not justified.

Examination of the efficiency of solar collectors

The experiment is the Vitosol 100, AP-20, 2 m^2 surface of Cu-based solar absorber optical efficiency of determining 800 W/m^2 of solar radiation intensity.

Solar collector efficiency:

$$\eta = \eta_0 - k_1 \frac{\Delta T}{E_g} - k_2 \frac{\Delta T^2}{E_g}, \tag{3.17}$$

$$\Delta T = T_m - T_a,\ T_m = T_{in} + \frac{T_e - T_{in}}{2},$$

where, T_m [K], average temperature of fluid, T_a [K], ambient air temperature, T_{in} [K], inlet temperature of fluid, T_e [K], outlet temperature of fluid, E_g [W/m^2], the global radiation, k_1, heat dissipation factor (thermal conductivity), k_2, heat loss coefficient (thermal radiation), η_0, optical efficiency. The comparative values of optical efficiency and heat dissipation factors of factory data based on: the case Vitosol 100, η_0= 81%, k_1 = 3,78 W/m^2K, k_2 = 0,013 W/m^2K^2.

Orientation measurements were carried out in advance. Expected amount of heat resulting from solar radiation this basis. I expected exploited by the amount of solar heat. So I determined the collector efficiency is considered to be a permanent feature during a given period.

Definition optical efficiency measurements and calculations

The test parameters (η_0) can not be measured directly, equal to the measured parameters were determined using extrapolation. The measured data can be found in Appendix F.1 of the paper.

Calculated from the data, data about the solar efficiency value of solar radiation 800 W/m^2, optical efficiency η_0 = 0,776. This value T_m-T_a = 0 line at the value of the maximum efficiency curve. The efficiency curve equation

written in Fig. 3.13 is shown. In the second instance on the basis of exponents in the equation of the first degree heat loss (thermal conductivity) characteristic value k_1 = 4,24 W/m^{2}K, a second-degree heat loss (radiation) typical value k_2 = 0,008 W/m^{2}K^2.

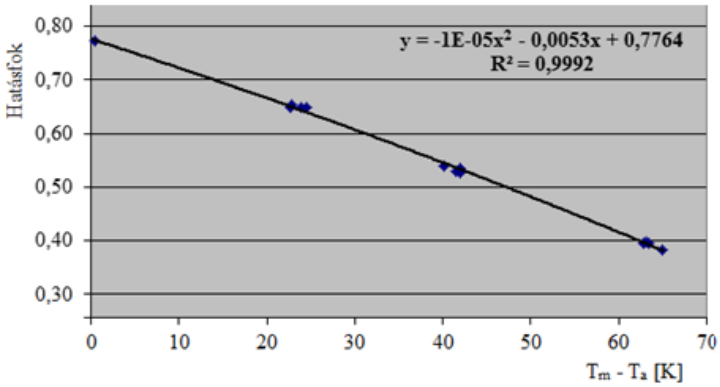

Fig. 3.13. Solar collector efficiency curve (I_g = 800 W/m^2)

The serial data (η_0 = 81%, k_1 = 3,78 W/m^{2}K, k_2 = 0,013 W/m^{2}K^2) by comparing the appropriate values, I have found that the values between the actual operating conditions are different in the direction of a few percentage points worse characteristics.

Efficiency range of the tile collector

The measured data of the tile collector, converge properly, according to the calculations of expected. Based on the data, the efficiency calculations were performed which shows that the values are within the area as shown in Fig. 3.14.

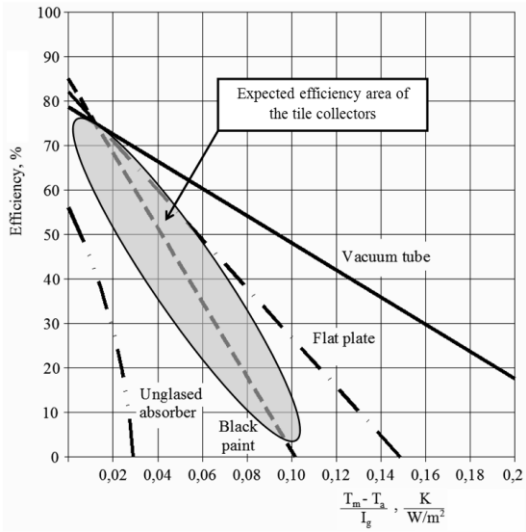

Fig. 3.14. Efficiency curves of different collectors

3.5. Process for refinement of solar collector efficiency curve

Temperature measurement accuracy has been examining the impact of the efficiency of the solar collectors accuracy. The given temperature ± 0,1 °C, ± 0,01 °C and ± 1 °C accuracy of reading inscribed in Fig. 3.15 graphically summarized the main features. The basic measurement accuracy of ± 0,1 °C. For optical efficiency of ± 0,01 °C accuracy given minimal difference. In addition to ± 1 ° C accuracy degrees difference in the optical effiency 0,01, in percent 1% (Fig. 3.15).

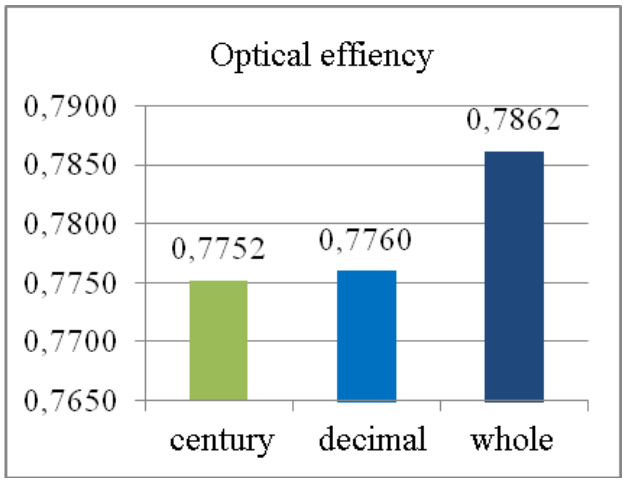

Fig. 3.15. Solar collector efficiency curves comparing accuracy

The results established the importance of carrying out mathematically and technically correct measurement instrumentation built next to the measurement accuracy.

3.6. Method for calculation of the solar collectors economy

In this paper I deal with the economies of the assessment of the calculation methods used. As an example, an earlier, 10-year-old investment appreciate. Analyse real energy price changes based on data up to 10 years for the plant life of the payback period.

Installation of solar collector hot water and heating

The following is based on 2003 completed solar project data, analysed the economic returns multiple calculation method.

Payback period without showing support:

$$M = B_k / Ny = 1\ 050\ 000 / 59\ 000 = 17{,}7 \text{ years.}$$

Future Value (FV) = savings (59 000) x 25 years = 1 475 000.- Ft

Net present value indicator:

NPV = PV(R)(=831 543) – PV(C)(=0) – PV(I)(=1 050 000) = - 218 457.- Ft

Yield-expense ratio:

BCR_1= PV(R) / (PV(I) + PV(C)) < 0 (~ 0,792) (PV(C) = 0.- Ft)

Payback time indicator 30% support:

$$M = B_k / Ny = 735\,000 / 59\,000 = 12{,}4 \text{ years.}$$

Future Value (FV) = savings (59 000) x 25 years = 1 475 000.- Ft

Net present value indicator:

NPV = PV(R)(=831 543) – PV(C)(=0) – PV(I)(=735 000) = 96 543.- Ft

Yield-expense ratio:

BCR_2= PV(R) / (PV(I) + PV(C)) = 1,13 (PV(C) = 0.- Ft).

Based on calculations made in 2003, the available data did not support financially the economics of the project.

The economic investment and operational experience rating:

The two most important change was the change in the price of electricity and natural gas. The average increase in the price of natural gas over 10 years (2004-2013) is 2.3 times, in the price of electricity is 1.5 times far as, respectively. The actual savings of ~ 107 320.- Ft/year is reduced, so without the support of the payback of 9,8 years, with support (30%) of 6,8 years.

Economic summary and recommendations

The preliminary financial analysis of the solar system, adverse, long-term returns indicated. However, the actual increase in energy prices significantly shortened it. The price of solar collector systems reduces the production development.

The improvements, efficiency of production processes are constantly evolving, so they can be observed decrease in the price. In addition to production costs, installation costs can be taken into account. The research and industry more and more attention is given to system integration, thus it is expected that installation costs will decline in the coming years.

5. NEW SCIENTIFIC RESULTS

New scientific results achieved during my research on a new type of solar collector and the optimal structure of the test are as follows:

1. Modelling of building integrated solar collectors

I have developed a physics-based mathematical model that can be used directly for modelling thermal collector element of the building process. The model of the building element collector layers of thermal and describing the mass transport-processes of differential equations linking were prepared with the help of the tile element temperature (T_t) and leaving liquid working fluid temperature (T_{out}) the following equations are introduced:

$$\dot{T}_t = \frac{I A_t + k_{ta} A_{ta} (T_a - T_t) - k_{wt} A_w (T_t - T_{out})}{c_t m_t}, \tag{4.1}$$

$$\dot{T}_{out} = \frac{k_{wt} A_w (T_t - T_{out}) - \dot{m}_w c_w (T_{out} - T_{in})}{c_w \rho_w V_w}. \tag{4.2}$$

The model was validated with a constructed tile collector measuring system. I found that the model can be reached on the elements surface temperature of about 0.5 ° C accuracy estimation.

2. The construction of building integrated solar collectors

The results of model simulations carried out on the basis of solar radiation energy attenuation measurements of the building materials, and I proposed the optimal form of tile elements, dimensions, forming part of the heat exchanger and its spatial location. I determined the distances to the pipe according to the original concrete tile format and the strength characteristics. Measurements using proved that the optimized tile elements constructed in accordance with an average operating solar collector, building integrated solar collectors.

3. Temperature distribution, and measurement data validation of building integrated solar collector

I proved that the panel temperature solar collectors field testing, modelling the values of the validation, the infrared camera sensor method is applicable.

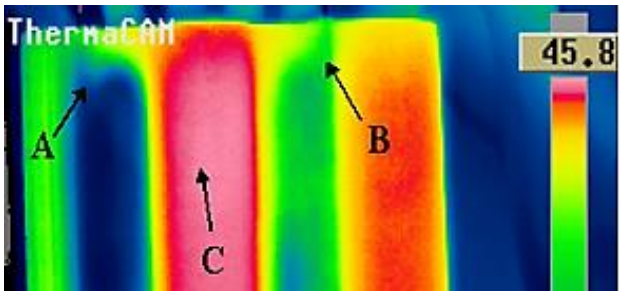

Fig. 4.1. Typical thermal areas of tile element

Based on the analysis of the recordings that the temperature of the tile elements measuring accuracy of 0.1 °C has an error lower priority (A - working fluid entry, B - working fluid exit, C - maximum temperature element tile) above as well. The method developed using the panel determined the collector temperature distribution is uneven, which helps optimize the structural development of the inventory items.

4. Definition of solar collectors efficiency curve

In doing so, the $X= (T_m-T_a)/G$ variable as a function of aggregate stated, the ambient temperature, the collector medium temperature and global radiation effect of the solar collector Efficiency. It developed the method, the single-glazed flat plate collectors with selective coating depending on the choice efficiency (η) at the following link and identifying the characteristics of the optical efficiency and losses coefficients:

$$\eta = -7{,}7693\ X^2 - 4{,}2225\ X + 0{,}7764.$$

The collector efficiency is introduced in addition to measured data fit the curve $D^2(X)= 0{,}9992$ variance value.

5. *Method for certification of accuracy of solar collector efficiency curve*

A new calculation method worked out without the use of efficiency curve to provide the high-precision measuring instruments. Proved on the basis of measured values of different measurement accuracy means that, compared to normal precision (±0.1 °C), the input data in the case of an order of magnitude greater (±0.01 °C), or an order of magnitude smaller (±1 °C) Accuracy respectively max. 0.014% and max. There is a 2.5% difference between the solar collector efficiency values of functions. The differential value of less than the initial value of the horizontal axis, the greater the difference in loss greater operating range.

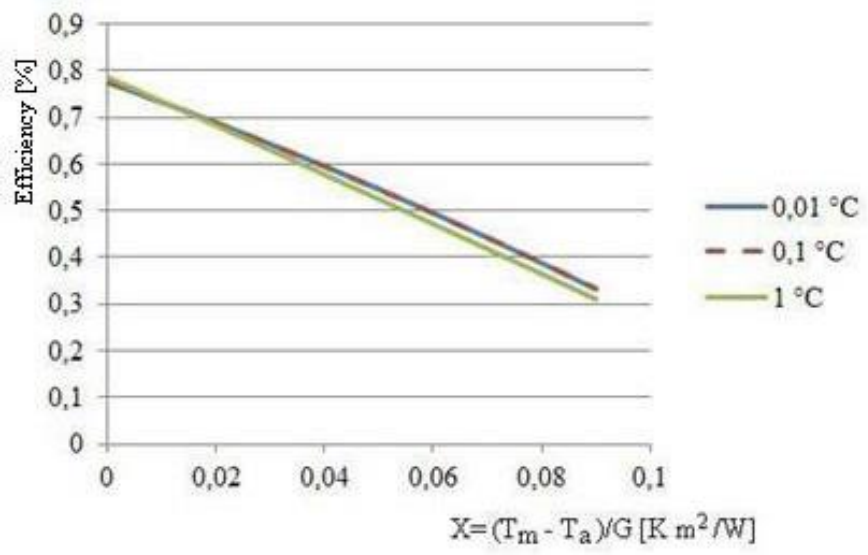

Fig. 4.2. Measurement accuracy the impact of the solar collector efficiency curve

6. Method for the calculation of the solar collectors economy

I developed a new method for the application of the economic characteristics of the solar collectors, calculate payback time. Based on the operating data for a long period of economic calculations proved the payback period of solar panels on the economics-based estimation methods currently used inaccuracy, application limitations.

The new calculation method developed taking into account the price of solar systems drop in their index, which is justified by the expansion of the European market for solar thermal systems. The investment will further improve the effectiveness of the assessment of external costs and the introduction of a proportional environmental impact factors.

The results of the new method of calculation show that the solar system within the technical lifetime of 20-25 years old, in contrast to the traditionally estimated payback periods of 15 to 18 years, based on actual data, for the same system, economically around the time of the investment recovered in 8-10 years.

6. CONCLUSIONS AND SUGGESTIONS

In today's high-rising pollution problems associated with sustaining economic growth. The renewable energy including solar energy available to all, decentralized exploitation could reduce it significantly.

In addition to today's efficiency-driven, but costly development concepts exploiting the necessary working less efficiently but cheaper options available. The design is simple and easy to assemble machines that are suitable for a specific period of solar radiation energy cost of capturing the first conclusions of the results of that structural element formed by collector items.

The studies and modelling in connection with the question arose of the currently used solar collector efficiency formula is suitable for the calculations. The medium in the solar collector when the temperature variable calculations, the change in the intensity of radiation affects the collector efficiency. The formula for calculating the efficiency of commonly used medium temperature solar collector does not fully reflect the real efficiency. The internal temperature distribution of solar collectors and ascertaining the impact of interconnected solar collectors on efficiency would be important for more precise control and improved energy-use.

I suggest the building's solar collectors element formed on the basis of results, in cases when it is incorporated into a conventional solar collectors due reference to aesthetic reasons. I also recommend these items to reduce the urban heat-island effect, when the heating of buildings worsens human comfort.

A commendable use of such protected architectural elements designed the renovation of buildings, increase the active utilization of solar energy in order to meet the increasingly stringent building energy standards.

Finally, I recommend the use of new techniques and solutions for the efficiency of solar collectors to ascertain the efficiency of subsequent carrying out checks, in addition to economic indicators correctly determining the forecast.

7. SUMMARY

Important to research and development activities for the capture and utilization of renewable forms of energy that led to the birth of applying them, and equipment, design of systems for the past two decades, commercially viable technologies.

I presented the active solar energy can be a new, non-standard, I have never used the possibility. The bodies of many collector thermal stratification developed a mathematical model of optimization and simulation experiments were carried out to establish. The investigation of the incident solar radiation energy characteristics of measurements were performed on samples of different surfaces. The equipment is designed based on the ideas, and we have built to meet expectations in the most options.

I studied the solar system efficiency of the method of calculation. The exact design measurements, using appropriate mathematical methods can be demonstrated that not only the high-precision instruments may be technically correct results are achieved certification. Not appropriate in some cases, the usual efficiency and accuracy of the formulas. it is definitely not light up some badly designed components, systems failures.

Economic calculations examined the possibility of investment in a given solar system parameters, economic return. In our country, the exploitation of solar energy are in good conditions. That is why we need to recognize these characteristics, advantages and disadvantages acknowledged described. Current economic indicators are not favorable for a rapid return, standard technology investment. It is important to take into account the direction of the price reduction systems in technical indicators, as well as protecting the environment, may feel a sense of responsibility for the future decision-making support.

In summary, noting the collector body shape and design of structural materials by changing, I can approach the maximum thermal efficiency is technically available. The design of the collector bodies of many thermal stratification of their modelling, simulation and measurement after the technically high quality manufacture, assemble, inexpensive, highly efficient collector bodies formed, right-lasting, economical systems can facilitate even greater use of solar energy.

8. MOST IMPORTANT PUBLICATIONS RELATED TO THE THESIS

Referred articles in foreign language

1. **Fekete, I.,** Farkas, I.: Thermal analysis of shell-structured solar collectors, Electrotehnica, Electronica, Automatica, Vol. 60, No. 2, 2012, pp. 43-48. ISSN 1582-5175
2. **Fekete, I.,** Farkas, I.: Factorial experiment method for determining the efficiency of solar collectors, Szent István University Faculty of Mechanical Engineering, Mechanical Engineering Letters, Gödöllő, Hungary, 2012, Vol. 8, pp. 38-52. HU ISSN 2060-3789
3. **Fekete, I.,** Farkas, I.: Numerical and experimental study of building integrated solar collectors, 2015, (publishing is in progress)

Referred articles in Hungarian language

4. **Fekete I.,** Farkas I.: Az építészeti alkalmazásokba integrálható héjszerkezetű kollektortestek, Magyar Energetika, XVIII. évf., 6. szám, 2011. november, 32-35. o. ISSN 1216-8599
5. **Fekete I.,** Farkas I.: Épületszerkezeti elemek szerepe a napenergia aktív hasznosításában, Mezőgazdasági Technika, LIII. évf., 2012. szeptember, 2-4. o. HU ISSN 0026 1890
6. **Fekete I.,** Farkas I.: Napkollektor gazdaságossága családi ház esetén, Energiagazdálkodás, 56. évf., 2-3. szám, 2015. június, 29-35. o. ISSN 0021-0757